

# A surface on the androgen receptor that allosterically regulates coactivator binding

Eva Estébanez-Perpiñá\*, Alexander A. Arnold†, Phuong Nguyen‡, Edson Delgado Rodrigues‡, Ellena Mar\*, Raynard Bateman§, Peter Pallai¶, Kevan M. Shokat§, John D. Baxter\*||, R. Kiplin Guy†, Paul Webb‡, and Robert J. Fletterick\*||

\*Department of Biochemistry and Biophysics, †Department of Molecular and Cellular Pharmacology, and ‡Diabetes Center and Department of Medicine, University of California, San Francisco, CA 94143; †Department of Chemical Biology and Therapeutics, St. Jude Children's Research Hospital, Memphis, TN 38105; and ¶Bioblocks, Inc., San Diego, CA 92121

Contributed by John D. Baxter, August 24, 2007 (sent for review May 12, 2007)

**Current approaches to inhibit nuclear receptor (NR) activity target the hormone binding pocket but face limitations. We have proposed that inhibitors, which bind to nuclear receptor surfaces that mediate assembly of the receptor's binding partners, might overcome some of these limitations. The androgen receptor (AR) plays a central role in prostate cancer, but conventional inhibitors lose effectiveness as cancer treatments because anti-androgen resistance usually develops. We conducted functional and x-ray screens to identify compounds that bind the AR surface and block binding of coactivators for AR activation function 2 (AF-2). Four compounds that block coactivator binding in solution with  $IC_{50} \approx 50 \mu M$  and inhibit AF-2 activity in cells were detected: three nonsteroidal antiinflammatory drugs and the thyroid hormone 3,3',5-triiodo-L-thyroacetic acid. Although visualization of compounds at the AR surface reveals weak binding at AF-2, the most potent inhibitors bind preferentially to a previously unknown regulatory surface cleft termed binding function (BF)-3, which is a known target for mutations in prostate cancer and androgen insensitivity syndrome. X-ray structural analysis reveals that 3,3',5-triiodo-L-thyroacetic acid binding to BF-3 remodels the adjacent interaction site AF-2 to weaken coactivator binding. Mutation of residues that form BF-3 inhibits AR function and AR AF-2 activity. We propose that BF-3 is a previously unrecognized allosteric regulatory site needed for AR activity *in vivo* and a possible pharmaceutical target.**

antagonist | high-throughput screening | regulatory surface | antiandrogens | nuclear receptors

Nuclear receptors (NRs) play widespread roles in disease and are major targets for pharmaceuticals (1), with many new compounds in development (2). Most NR ligands interact with the internal ligand binding pocket [binding function (BF) 1] in the C-terminal ligand binding domain (LBD) core (3). From here, the ligands modulate NR activity by allosterically reshaping the LBD surface, with concomitant effects on coregulator association and gene expression (3–6). It remains conceivable that ligands could bind elsewhere. We identified a compound that binds to the TR dimer interaction surface (7), we and others identified compounds that bind the NR activation function 2 (AF-2) surface (discussed below), and another group showed that glucose and oxysterols cooperate in activation of liver X receptors (8).

The strategy of targeting the ligand binding pocket with pharmaceuticals has limitations. First, ligand size can be limited by the enclosed nature of the pocket (3). Second, it is difficult to devise strategies to modulate interaction surfaces that are not remodeled by ligand or orphan NRs that lack known ligands or ligand binding cavities. Third, partial agonist or mixed agonist activities of ligands that bind BF-1 may not be desirable. This is a particular problem for androgen receptor (AR) and estrogen receptor antagonists, which are used to treat, respectively, hormone-dependent prostate and breast cancers but can become ineffective and promote tumor growth (9–11).

In principle, pharmaceutical attack at NR surface active sites could overcome these problems (12), and NR AF-2 is a particularly attractive drug target (13). AF-2 is formed in response to agonist binding and binds coregulators, including the steroid receptor coactivator (SRC) family. Only 6–8 amino acids in AF-2 are crucial, and these form a hydrophobic cleft that binds short  $\alpha$ -helical peptides (NR boxes) in target coactivators and could bind small molecules (BF-2). We identified two compounds that block thyroid hormone receptor AF-2 association with coactivators in solution and receptor activity in cells (14). Others identified estrogen receptor-interacting compounds, some of which block coregulator binding *in vitro* (14–17).

Strategies that target AR AF-2 could yield new therapeutics for prostate cancer and other conditions (18–22). AR AF-2-interacting peptides inhibit androgen response, representing proof of principle that intervention at this surface is a viable strategy for inhibition of AR activity *in vivo* (18). Compounds that bind AF-2 should inhibit intramolecular association between the AR LBD and N-terminal domain (23) required for optimal AR responses at many target genes and interactions with coregulators that participate in AR action such as AR-associated protein 70 (ARA70) and SRC2 (20). AR AF-2 binds short  $\alpha$ -helical peptides with consensus FXXLF and the more common NR consensus LXXLL. Our x-ray structures of AR LBD with representative peptides reveal that AF-2 amino acid side chains move to create deep pockets that accommodate the bulky aromatic amino acid side chains and represent attractive targets for small molecules (19, 20, 24). These conformational changes nevertheless also make it difficult to rationally design drugs that bind this protein interaction surface (25).

Author contributions: E.E.-P., A.A.A., J.D.B., R.K.G., P.W., and R.J.F. designed research; E.E.-P., A.A.A., P.N., E.D.R., E.M., and P.W. performed research; E.E.-P., A.A.A., P.N., E.D.R., R.B., P.P., K.M.S., R.K.G., and P.W. contributed new reagents/analytic tools; E.E.-P., A.A.A., P.N., J.D.B., R.K.G., P.W., and R.J.F. analyzed data; and E.E.-P., A.A.A., J.D.B., R.K.G., P.W., and R.J.F. wrote the paper.

Conflict of interest statement: J.D.B. has proprietary interests in and serves as a consultant to Karo Bio AB, which has commercial interests in the nuclear receptor field.

Freely available online through the PNAS open access option.

Abbreviations: AF-2, activation function 2; AR, androgen receptor; BF, binding function; DHT, dihydrotestosterone; FLF, flufenamic acid; FP, fluorescence polarization; K10, 1-tert-butyl-3-(2,5-dimethyl-benzyl)-1H-pyrazolo[3,4-d]pyrimidin-4-ylamine; LBD, ligand-binding domain; 2MI, 2-methylindole; NR, nuclear receptor; RB1, 3-((1-tert-butyl-4-amino-1H-pyrazolo[3,4-d]pyrimidin-3-yl)methyl)phenol; SRC, steroid receptor coactivator; TOL, tofenamic acid; Triac, 3,3',5-triiodo-L-thyroacetic acid; T<sub>3</sub>, triiodothyronine; UCSF, University of California, San Francisco.

Data deposition: The atomic coordinates and structure factors have been deposited in the Protein Data Bank, www.pdb.org (PDB ID codes 2PIO, 2PIP, 2PIQ, 2PIR, 2PIT, 2PIU, 2PIV, 2PIW, 2PIX, 2PKL, and 2QPY).

||To whom correspondence may be addressed. E-mail: jbxater918@aol.com or flett@cgl.ucsf.edu.

This article contains supporting information online at [www.pnas.org/cgi/content/full/0708036104/DC1](http://www.pnas.org/cgi/content/full/0708036104/DC1).

© 2007 by The National Academy of Sciences of the USA



to activation domains from VP16 and CBP, confirming that effects are not related to toxicity (data not shown).

**X-Ray Screens Reveal AR-Interacting Molecules at AF-2 and a New Site (BF-3).** We also performed structural screens for AR-interacting compounds (32). AR LBD-DHT crystals were soaked with individual chemicals in groups of 1–10, and interacting compounds were localized by x-ray diffraction and visual inspection of electron densities (SI Table 2). Soaks were performed with the Prestwick library mentioned above and two libraries of chemical fragments that are unlikely to bind the AR with high affinity but were nonetheless chosen for their potential to be linked or modified to create tighter binding scaffolds. One library, assembled at the University of California, San Francisco (UCSF), comprises 400 protein kinase inhibitors and related compounds with characteristics of heterocyclic rings, similar to side chains of FXXLF motifs. The second is a proprietary library of 200 chemicals with multiple functionalities (BioBlocks).

We found seven drugs at the AR surface. From the Prestwick library we detected FLF, Triac, and T<sub>3</sub> (also identified in solution screens). We could not assess TOL and meclofenamic acid binding because these compounds disrupt AR crystals and it was possible to obtain FLF data sets only with short soaks (15 min). We also detected four compounds from the UCSF library (Fig. 1B). 1-*tert*-butyl-3-(2,5-dimethyl-benzyl)-1H-pyrazolo[3,4-*D*]pyrimidin-4-ylamine (K10) and 3-((1-*tert*-butyl-4-amino-1H-pyrazolo[3,4-*D*]pyrimidin-3-yl)methyl)phenol (RB1) are kinase inhibitors with two aromatic rings; 2-methylindole (2MI) and indole acetic acid resemble tryptophan indole rings. None of the UCSF library compounds promotes SRC2–3 dissociation in FP assays (data not shown), as expected from library design of probable low-affinity binders.

Unexpectedly, the compounds that displace SRC2–3 from AF-2, FLF, Triac, T<sub>3</sub>, and two low-affinity compounds, 2MI and indole-3-carboxylic acid, bind to a previously unknown site, BF-3 (Fig. 3). This is a hydrophobic cleft at the junction of H1, the H3–H5 loop, and H9 that is almost as large as AF-2 and exhibits characteristics of protein interaction surfaces (developed below).

None of the compounds appear at AF-2 in short soaks, but Triac, T<sub>3</sub>, 2MI, and kinase inhibitors K10 and RB1 eventually appeared at this location with soaks of 7–20 h. FLF damages AR crystals at these times. Slow appearance of small molecules at AR AF-2 is not related to inaccessibility; crystal soaks with SRC2–3 peptide revealed electron density corresponding to the LxxLL motif at AF-2 within 1 h (data not shown).

Together, the studies confirm that it is feasible to detect AR surface-interacting compounds with x-ray screens, that small molecules bind AF-2, and, surprisingly, a novel small molecule binding site, BF-3.

**AR Surface-Interacting Compounds Bind Preferentially to BF-3.** X-ray structures suggest that Triac interacts preferentially at BF-3 vs. AF-2 (Fig. 4 and SI Table 3). Triac covers 580 Å<sup>2</sup> of both surfaces yet exhibits stronger, uniformly well defined electron density at BF-3; the Triac proximal and distal phenyl rings make hydrophobic contacts with a large BF-3 surface comprising Pro-723, Phe-673, and Ile-672 from H1, Gly-724 and Asn-727 from H3–5, and Phe-826, Glu-829, Glu-837, Arg-840, and Asn-833 from H9 (Fig. 4 A and C). In addition, the distal phenyl ring hydroxyl group hydrogen-bonds with Asn-727, and the proximal phenyl ring carboxylate hydrogen-bonds with the oppositely charged Arg-840 side chain. Weaker association at AF-2 is due to poor fit (Fig. 4 D and F). The Triac distal ring is well defined and makes hydrophobic contacts with a deep AF-2 subpocket (S1) that hosts F<sub>1</sub> or L<sub>1</sub> of the signature motif F<sub>1</sub>XXL<sub>4</sub>F<sub>5</sub>/L<sub>1</sub>XXL<sub>4</sub>L<sub>5</sub>, but the proximal phenyl ring is poorly defined and spans the S2 and S3 subsites that host L<sub>4</sub> and F<sub>5</sub>/L<sub>5</sub> (Fig. 4D). T<sub>3</sub> displayed similar binding modes to Triac at both sites (data not shown).

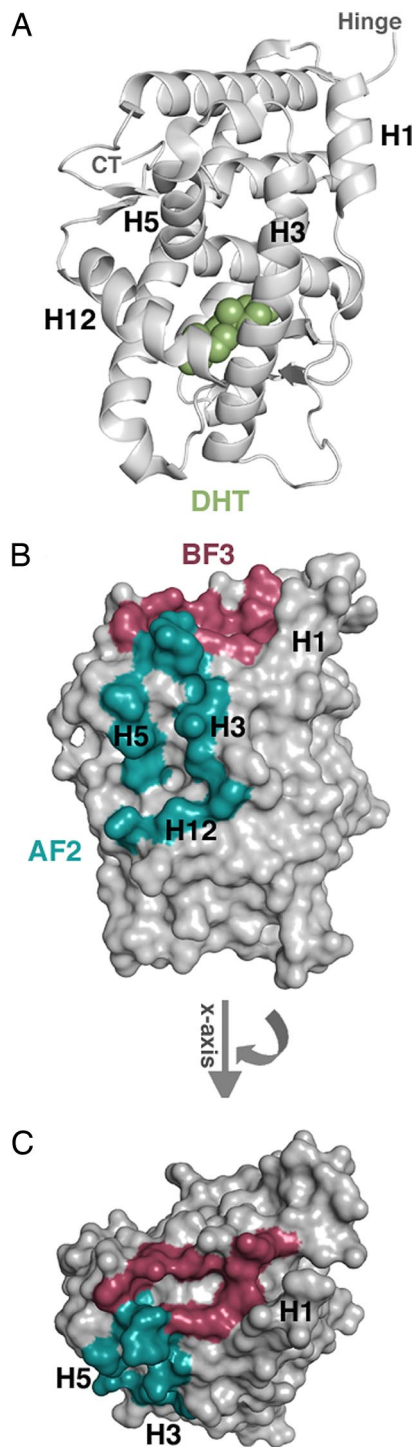


**Fig. 3.** AF-2 and BF-3. (A) Schematic of AR LBD showing location of DHT, key AF-2 helices 3, 5, and 12, and H1. (B) Space-filling model showing residues in AF-2 (cyan) and BF-3 (red). (C) As in B, rotated 90° to reveal BF-3.

Interactions at BF-3 are well defined for other compounds. FLF aromatic rings interact tangentially with BF-3 to bury 520 Å<sup>2</sup> of solvent-exposed surface (Fig. 4 B and C). Whereas 2MI displays a binding mode similar to the Triac distal phenyl ring and buries, respectively, 280 Å<sup>2</sup> and 370 Å<sup>2</sup> of accessible BF-3 and AF-2 surfaces, it is better resolved at BF-3 (data not shown). Indole-3-carboxylic acid binds BF-3 in a similar mode to 2MI and also appears well defined (data not shown). By contrast, K10 and

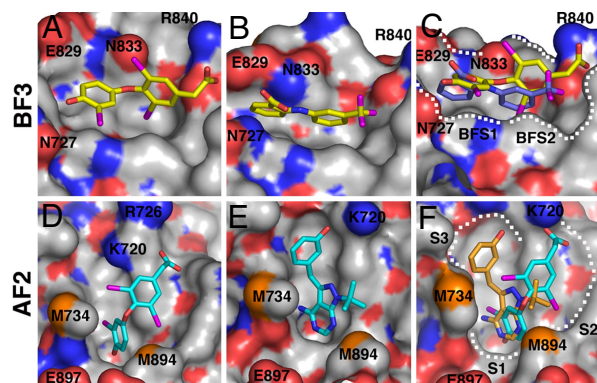


**Fig. 4.** Interactions at the AR LBD surface. (A–C) BF-3 including Glu-829, Asn-833, Arg-840, Phe-673, and Tyr-834 is highlighted by dots and divided into two subpockets that accommodate Triac and FLF phenolic rings. Basic residues are in blue, and acidic residues are in red. Shown are close-ups of interactions with Triac (A) and FLF (B) as yellow stick models. (C) Superimposed Triac (yellow) plus FLF (dark blue). (D–F) AF-2 lined by Met-734, Lys-720, Glu-897, and Met-894 with subsites (S1–S3) highlighted by dots. Basic residues are in blue, acidic residues are in red, and Met is in yellow. D and E show close-ups of Triac and RB1, respectively. (F) Superimposed Triac (blue) plus RB1 (orange). Triac interacts with S1 and the area between S2 and S3 whereas RB1 interacts with S1 and S3.

RB1 occupy  $\approx 580 \text{ \AA}^2$  of solvent-exposed AF-2 surface but exhibit even weaker electron density than Triac (Fig. 4 E and F and data not shown). Both compounds engage in hydrophobic interactions with S1 and S3, with better definition at S1 (Fig. 4F).

**Interactions at BF-3 Weaken Coactivator Binding.** Comparison of the AR surface with or without Triac, T<sub>3</sub>, and FLF reveals structural alterations. Four BF-3 residues (Arg-840, Asn-727, Phe-826, and Glu-829) that point out of the pocket into solution point inward and engage the compound (Fig. 5A). This is accompanied by large movements of the Arg-726 side chain, close to AF-2, and repositioning of AF-2 residues Lys-717 and Met-734 (data not shown). There are also small but significant shifts in secondary structural elements; residues 720–730 (H3) and 825–847 (H9) exhibit rmsd of 0.33 and 0.44, respectively. Thus, Triac and FLF promote structural rearrangements in BF-3 that are propagated to AF-2.

Drug interactions at BF-3 cause coregulator peptides that are bound to AF-2 to become disordered. In crystals of ternary complexes of AR LBD-DHT-SRC2-3 (LXXLL) and AR LBD-DHT-ARA70 (FXXLF), the peptides fold into  $\alpha$ -helices of 15 and 9 amino acids (20), respectively, clearly defined by electron density (Fig. 5A Right and B Right). Short Triac incubations result in loss of electron density in the regions that flank SRC2-3 hydrophobic triads (Fig. 5A) and disruption of Arg-726 interactions with SRC2-3 residues that lie C-terminal to the LxxLL motif. Triac binding to BF-3 also weakened ARA70 FxxLF contacts (Fig. 5B); only four residues are visible with Leu+4 and Phe+5 completely defined (Fig. 5B Right). Arg-726 does not contact the FXXLF peptide, suggesting that reorganization of AF-2 itself is important for this effect. Unexpectedly, Arg-840 adopts the inward-facing conformation in this experiment (Fig. 5B). Similar Arg-840 rearrangements are also seen with artificial FXXLF peptides (19), suggesting that it is a hitherto unappreciated feature of AR interactions with these NR boxes. It is unlikely that Triac interacts directly with AF-2 to disrupt coactivator binding, because it is not detected at AF-2 at these times and the electron-rich iodine groups of Triac represent particularly good markers. Control soaks with solvent (DMSO) reveal no similar effects on coregulator peptide organization (data not

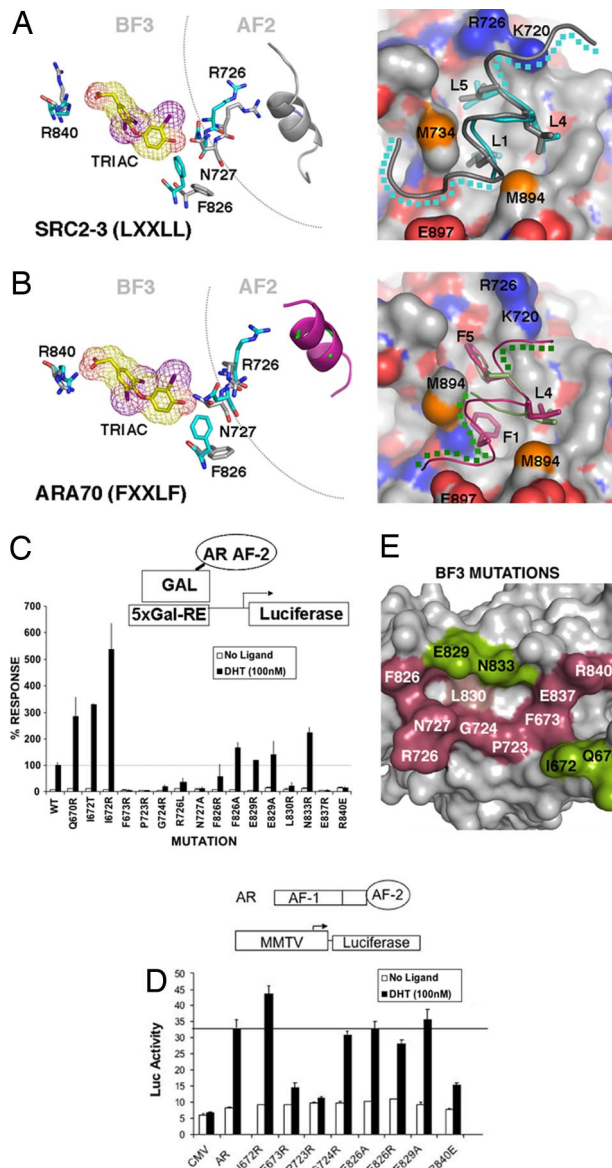


**Fig. 5.** BF-3 modulates AF-2. (A) Superposition of AR with SRC2-3 with Triac (blue sticks), without Triac (gray sticks), and with Triac with no peptide (yellow sticks). Arg-840, Phe-826, Asn-727 (BF-3), and Arg-726 (AF-2) adopt different conformations. Without Triac, Arg-840 points outward and Arg-726 contacts SRC2-3 (gray). With Triac, Arg-840 contacts ligand and Arg-726 does not contact SRC2-3 (blue). (Right) SRC2-3 without Triac (gray trace) and with Triac (blue trace). Blue dots indicate regions not visible with Triac; Leu residues are shown as sticks. (B) As in A, with ARA70 with Triac (blue) and without Triac (gray). Reorganization is similar to A except that Arg-840 points inward without Triac. (C) AR AF-2 assay; wild type = 100%. Results are averages of at least three different experiments. (D) Transfection with full-length AR active at MMTV-Luc. (E) BF-3 defined by mutagenesis. Raspberry, residues needed for activity; green, mutations that increase activity.

shown). Thus, Triac interactions at BF-3 weaken contacts between AR and coactivator peptides.

If BF-3 is important for AR action, then BF-3 mutations should alter AR activity. Mutations at Gln-670, Ile-672, and Leu-830 are associated with prostate cancer (33–35). Leu-830, Pro-723, Gly-724, and Arg-840 are mutated in androgen insensitivity syndrome (36) ([www.androgendb.mcgill.ca](http://www.androgendb.mcgill.ca)). Targeted mutagenesis of Asn-727 and Arg-840, which move on Triac binding, eliminate AR LBD activity (Fig. 5C), similar to inhi-

bition obtained with mutations in AF-2 (20). Likewise, mutations at Phe-673, Pro-723, Glu-724, Glu-737, and, possibly, Arg-726 and Phe-826 reduce activity. Mutations in nearby residues, Gln-670, Ile-672, Glu-829, and Asn-833, increase AR AF-2 activity up to 5-fold. Similar results were obtained with full-length AR at MMTV-LUC; mutations at Phe-673, Pro-723, and Arg-840 inhibited androgen response (Fig. 5D). The mutations that inhibit AR activity describe a continuous patch that resembles the BF-3 surface defined by chemical interactions (Fig. 5E).

BF-3 could be present in other NRs. Part of the site, the H3–H4 loop, is a signature sequence (37). Superposition of published structures reveals conservation of BF-3 residues in the steroid subfamily (SI Fig. 6). Mutations in equivalent regions of estrogen and glucocorticoid receptor are implicated in coactivator binding (38, 39). Collectively, these data provide evidence for a role of BF-3 in NR action.

## Discussion

We used two screens to identify molecules that inhibit AR activity by binding the AR LBD surface at important sites. FP screening detects four drugs that inhibit SRC2–3 peptide binding with  $IC_{50} \approx 50 \mu\text{M}$  in a library of 55,000 compounds (FLF, TOL, meclofenamic acid, and Triac).  $T_3$  was identified on the basis of its similarities to Triac. X-ray screening of three small compound libraries (Prestwick, UCSF kinase inhibitors, and BioBlocks) detected seven compounds, including three that were identified in functional screens (FLF, Triac, and  $T_3$ ) and new compounds (RB1, K10, 2MI, and indole-3-carboxylic acid).

Our most surprising finding is that the best inhibitors interact preferentially with a novel surface site (BF-3). Three lines of evidence suggest that ligand interactions with BF-3 exert indirect effects on AF-2 to inhibit coregulator binding. First, FLF and Triac promote reorganization of BF-3 residues (Asn-727, Phe-826, Glu-829, and Arg-840) and AF-2 residues (Met-734 and Lys-717) and large-scale repositioning of Arg-726 at the AF-2 boundary. Second, short Triac soaks weaken AR interactions with FXXLF and LXXLL peptides in AR-DHT-NR box crystals. Third, BF-3 residues are required for optimal AR AF-2 activity in cell culture. We considered the possibility that compounds displace SRC2–3 through weak interactions with AF-2. In this case, rapid binding of compounds to BF-3 may reflect crystal packing constraints that render BF-3 available for drug interactions. We believe that this is unlikely because a bulky SRC2–3 peptide appears rapidly at AR AF-2 in crystal soaks (data not shown), but we cannot yet rule out this possibility. The models are not mutually exclusive; BF-3-dependent effects could complement weak binding of compounds to AF-2.

The natural role of BF-3 *in vivo* is unknown, but our data, coupled with natural mutations, suggest that the site is important. Mutations at Gln-670, Ile-672, and Leu-830 enhance AR action in prostate cancer (33, 35, 40), and mutations at Gln-670 and Ile-672 enhance AR AF-2 activity (Fig. 5C). BF-3 is a target for androgen insensitivity syndrome mutations at Ile-672, Leu-830, Arg-840, and Asn-727, with mutations in the latter two diminishing SRC2 binding *in vitro* although neither contacts coregulator (41). Finally, mutations in BF-3 of other NRs are implicated in coactivator binding (38, 42). BF-3 could bind regulatory proteins or other AR domains and could, for example, communicate information about DNA binding domain position to the LBD and AF-2 and vice versa.

Regardless of the mechanism by which compounds displace SRC2–3, the fact that we detect such compounds for ARs and TRs (14) suggests that functional and structural screens are viable methods for NR inhibitor development. High-throughput functional screens detect inhibitors among large libraries of drug-like compounds, and our experience with ARs and TRs suggests that “hits” are uncommon but are specific and rarely

false positives. It is not feasible to perform high-throughput x-ray screens with large libraries, but this method complements functional screens in three ways. First, x-ray screens provide information about binding of leads. For example, Triac, RB1, and K10 interact preferentially with AF-2 S1, so strategies to improve binding to S2 or S3 would yield higher-affinity compounds. Second, x-ray screening reveals unexpected sites or interaction modes; the discovery of BF-3 was a surprise. Third, x-ray screens are the only known method to identify weakly interacting compounds that bind the surface with high ligand efficiency and comprise building blocks for tight binding compounds.

It may be feasible to develop three types of small molecules that modulate AR and NR activity: classical drugs that bind BF-1, drugs that bind surface-exposed active sites such as AF-2, or drugs that bind surface allosteric sites such as BF-3. This greatly expands the number of NR pharmaceutical targets and the potential spectrum of responses, and representatives of each class could even be used together. The fact that three leads are off-patent aspirin derivatives approved for human use (30), and that others are thyroid hormones with known actions in humans, raises the possibility that such compounds could be used for prostate cancer treatment. It is unlikely that natural  $T_3$  or Triac concentrations approach levels required to bind the AR surface *in vivo* (31), but it is intriguing to speculate that AR surface interactions contribute to documented inhibitory effects of nonsteroidal antiinflammatory drugs on growth and survival of prostate cancer cells (43). We propose that well designed compounds engaging AF-2 or BF-3 will modulate coregulator recruitment in physiological settings, including cancer, and that combined functional/x-ray screening is a useful strategy for identification of ligands that act at NR surfaces.

## Materials and Methods

**Peptide Synthesis.** Five milligrams of SRC2–3 (CKENALLRYL-LDKDD) was dissolved in 1 ml of PBS and added to 50 mg of 5-iodoacetamidofluorescein in 1 ml of DMF. After 3 h at room temperature, 0.5 ml of ethanethiol was added and peptide was purified by HPLC [XTerra C18 column: A, water (0.05% TFA); B, CH<sub>3</sub>CN (0.05% TFA), linear gradient 0100% over 25 min; Waters]. Evaporation of fractions gave 3.8 mg of labeled peptide. Mass analysis (MALDI-TOF) showed one species at 2,195.8 (*m/z*).

**Protein Expression.** AR LBD (residues 663–919) was expressed in *Escherichia coli* in the presence of DHT and purified by using published protocols (20). Functionality was determined by SRC2–3 binding in FP assays (20);  $K_d$  for SRC2–3 binding was 2.7  $\mu\text{M}$ .

**Solution Screening.** Plates (384 wells; Costar 3710) were prepared with 4  $\mu\text{l}$  of compound (5 mM in DMSO) plus 80  $\mu\text{l}$  of dilution buffer (20 mM Tris-HCl/100 mM NaCl, pH 7.2/1 mM DTT/1 mM EDTA/0.01% Nonidet P-40/10% glycerol/10.5% DMSO) by using a WellMate (Matrix). Five microliters from the dilution plates was transferred to 384-well assay plates followed by 20  $\mu\text{l}$  of protein mixture (6.25  $\mu\text{M}$  AR plus DHT and 0.0125  $\mu\text{M}$  peptide in dilution buffer; final concentration 50  $\mu\text{M}$  compound, 4% DMSO). FP was measured after 2 h (excitation  $\lambda$  485 nm, emission  $\lambda$  530 nm) on an AD plate reader (Molecular Devices). Longer incubation times led to inhibition of FP in negative controls (DMSO only), possibly reflecting AR instability. For dose–response, compounds were diluted from 5,000 to 2.44  $\mu\text{M}$  in DMSO into a 96-well plate (Costar 3365). Twenty microliters of mixture was added to 1.2  $\mu\text{l}$  of compounds in 384-well plates (Costar 3710), yielding a final concentration of 300 to 0.146  $\mu\text{M}$ , and equilibrated for 5 h before FP. Data were analyzed by using SigmaPlot 8.0 (SPSS, Chicago, IL), and  $K_d$  values were obtained by fitting data to  $y = \text{minimum} + (\text{maximum} - \text{minimum})/1 + (x/K_d)$  Hill slope.

**Library Assembly for X-Ray Screens.** Three libraries with different characteristics were used. A commercial library of 1,120 FDA-approved drugs was from Prestwick. Compounds with protein kinase inhibitor characteristics or multiple heterocyclic rings were from UCSF. Two hundred small compounds <200 Da with druglike character, designed as building blocks for larger molecules, were from BioBlocks.

**X-Ray Screening.** Compounds were dissolved in DMSO at 10–20 mM and soaked with AR:DHT crystals on 96-well plates. Typically, a drop with one to four AR crystals is soaked with 1–10 compounds. Increasing 0.2  $\mu$ l units of compound are added, and crystals are monitored. If crystals survive, another 0.2  $\mu$ l is added until crystals show fatigue. Fresh crystals plus maximum tolerated chemical volume were used for cryo treatment and freezing.

**Crystallization, Structure Determination, and Refinement.** Approximately 80 crystals were flash-cooled in liquid N<sub>2</sub> for analysis at the Lawrence Berkeley National Laboratory Advanced Light Source (beamline 8.3.1) in each trip. Only data sets from crystals that diffract <2.5 Å were collected. All compounds that cause AR LBD crystals to diffract poorly were checked afterward, and soaks with lower concentration were performed. Data sets from 35 crystals were measured per 8-h shift and indexed and merged by using ELVES. Molecular replacement solutions were obtained by using rotation and translation functions from CNS

software. Model building used QUANTA (Accelrys Software) monitored by using free *R* factor. Visual inspection of electron densities using QUANTA allows identification of interacting compounds. A composite omit map was also calculated absent 5% of the molecule to remove model bias. Calculation of electron density and crystallographic refinement was performed with CNS by using target parameters of Engh and Huber. Several cycles of model building, conjugate gradient minimization, and simulated annealing resulted in structures with good stereochemistry. A Ramachandran plot shows that most residues fall into favored regions (SI Table 2).

**Pull-Downs and Transfections.** Vectors, expression and labeling, and assay procedures were previously described (20). New mutants were made by QuikChange Site-Directed Mutagenesis (Stratagene).

We thank Pascal Egea, Elena Sablin, Anang Shelat, and Arnold T. Hagler for discussions; James Holton and George Meigs for assistance at the Advanced Light Source (beamline 8.3.1); and Chao Zhang (UCSF) for K10. This work was supported by the Prostate Cancer Foundation (R.J.F. and P.W.); National Institutes of Health Grants DK58080 (to R.J.F. and R.K.G.), DK41482 (to J.D.B.), and DK51281 (to J.D.B.); Specialized Programs of Research Excellence/National Cancer Institute Grant CA89520 (to E.E.-P.); Department of Defense Grants W81XWH-05-1-0545 (to R.J.F.) and PC030607 (to P.W.); the UCSF Prostate Cancer Program (P.W.); and a Herbert Boyer Postdoctoral Fellowship (to E.E.-P.).

- Laudet V, Gronemeyer H (2002) *The Nuclear Receptor Facts Book* (Academic, London).
- Baxter JD, Goede P, Apriletti JW, West BL, Feng W, Mellstrom K, Fletterick RJ, Wagner RL, Kushner PJ, Ribeiro RC, et al. (2002) *Endocrinology* 143:517–524.
- Weatherman RV, Fletterick RJ, Scanlan TS (1999) *Annu Rev Biochem* 68:559–581.
- Nettles KW, Greene GL (2005) *Annu Rev Physiol* 67:309–333.
- Rosenfeld MG, Lunyak VV, Glass CK (2006) *Genes Dev* 20:1405–1428.
- Lonard DM, O'Malley BW (2006) *Cell* 125:411–414.
- Borngraeber S, Budny MJ, Chiellini G, Cunha-Lima ST, Togashi M, Webb P, Baxter JD, Scanlan TS, Fletterick RJ (2003) *Proc Natl Acad Sci USA* 100:15358–15363.
- Mitro N, Mak PA, Vargas L, Godio C, Hampton E, Molteni V, Kreusch A, Saez E (2007) *Nature* 445:219–223.
- Dehm SM, Tindall DJ (2006) *J Cell Biochem* 99:333–344.
- Lewis-Wambi JS, Jordan VC (2005) *Breast Dis* 24:93–105.
- Scher HI, Sawyers CL (2005) *J Clin Oncol* 23:8253–8261.
- Darimont BD (2003) *Chem Biol* 10:675–676.
- Feng W, Ribeiro RC, Wagner RL, Nguyen H, Apriletti JW, Fletterick RJ, Baxter JD, Kushner PJ, West BL (1998) *Science* 280:1747–1749.
- Arnold LA, Estebanez-Perpina E, Togashi M, Jouravel N, Shelat A, McReynolds AC, Mar E, Nguyen P, Baxter JD, Fletterick RJ, et al. (2005) *J Biol Chem* 280:43048–43055.
- Arnold LA, Estebanez-Perpina E, Togashi M, Shelat A, Ocasio CA, McReynolds AC, Nguyen P, Baxter JD, Fletterick RJ, Webb P, Guy RK (2006) *Sci STKE* 2006:pl3.
- Wang Y, Chirgadze NY, Briggs SL, Khan S, Jensen EV, Burris TP (2006) *Proc Natl Acad Sci USA* 103:9908–9911.
- Rodriguez AL, Tamrazi A, Collins ML, Katzenellenbogen JA (2004) *J Med Chem* 47:600–611.
- Chang CY, Abdo J, Hartney T, McDonnell DP (2005) *Mol Endocrinol* 19:2478–2490.
- Hur E, Pfaff SJ, Payne ES, Gron H, Buehrer BM, Fletterick RJ (2004) *PLoS Biol* 2:E274.
- Estebanez-Perpina E, Moore JM, Mar E, Delgado-Rodriguez E, Nguyen P, Baxter JD, Buehrer BM, Webb P, Fletterick RJ, Guy RK (2005) *J Biol Chem* 280:8060–8068.
- Chang CY, McDonnell DP (2005) *Trends Pharmacol Sci* 26:225–228.
- Heinlein CA, Chang C (2004) *Endocr Rev* 25:276–308.
- He B, Wilson EM (2002) *Mol Genet Metab* 75:293–298.
- He B, Gampe RT, Jr, Kole AJ, Hnat AT, Stanley TB, An G, Stewart EL, Kalman RI, Minges JT, Wilson EM (2004) *Mol Cell* 16:425–438.
- Wells J, Arkin M, Braisted A, DeLano W, McDowell B, Oslob J, Raimundo B, Randal M (2003) *Ernst Schering Res Found Workshop* 19–27.
- Arkin MR, Wells JA (2004) *Nat Rev Drug Discovery* 3:301–317.
- Berg T (2003) *Angew Chem Int Ed Engl* 42:2462–2481.
- Toogood PL (2002) *Curr Opin Chem Biol* 6:472–478.
- Vassilev LT, Vu BT, Graves B, Carvajal D, Podlaski F, Filipovic Z, Kong N, Kammlott U, Lukacs C, Klein C, et al. (2004) *Science* 303:844–848.
- Flower R (2003) *Nat Rev Drug Discovery* 2:179–191.
- Braverman LE, Utiger RD (2000) (Lippincott Williams & Wilkins, Philadelphia).
- Nienaber VL, Richardson PL, Klinghofer V, Bouska JJ, Giranda VL, Greer J (2000) *Nature* 18:1105–1108.
- Buchanan G, Yang M, Harris JM, Nahm HS, Han G, Moore N, Bentel JM, Matusik RJ, Horsfall DJ, Marshall VR, et al. (2001) *Mol Endocrinol* 15:46–56.
- Buchanan G, Greenberg NM, Scher HI, Harris JM, Marshall VR, Tilley WD (2001) *Clin Cancer Res* 7:1273–1281.
- Shi XB, Ma AH, Xia L, Kung HJ, de Vere White RW (2002) *Cancer Res* 62:1496–1502.
- McPhaul MJ (2002) *Mol Cell Endocrinol* 198:61–67.
- Brelivet Y, Kammerer S, Rochel N, Poch O, Moras D (2004) *EMBO Rep* 5:423–429.
- Tanenbaum DM, Wang Y, Williams SP, Sigler PB (1998) *Proc Natl Acad Sci USA* 95:5998–6003.
- Milhon J, Lee S, Kohli K, Chen D, Hong H, Stallcup MR (1997) *Mol Endocrinol* 11:1795–1805.
- Chavez B, Vilchis F, Zenteno JC, Larrea F, Kofman-Alfaro S (2001) *Clin Genet* 59:185–188.
- Lim J, Ghadessy FJ, Abdullah AA, Pinsky L, Trifiro M, Yong EL (2000) *Mol Endocrinol* 14:1187–1197.
- Milhon J, Lee S, Kohli K, Chen D, Hong H, Stallcup MR (1997) *Mol Endocrinol* 11:1795–1805.
- Andrews P, Krygier S, Djakiew D (2002) *Cancer Chemother Pharmacol* 49:179–186.